



RESEARCH ARTICLE

Low-frequency rTMS targeting individual self-initiated finger-tapping task activation modulates the amplitude of local neural activity in the putamen

Jue Wang¹  | Xin-Ping Deng^{2,3,4} | Yun-Song Hu^{2,3,4} | Juan Yue^{2,3,4} | Qiu Ge^{2,3,4} | Xiao-Long Li^{2,3,4} | Zi-Jian Feng^{2,3,4} 

¹Institute of Sports Medicine and Health, Chengdu Sport University, Chengdu, People's Republic of China

²Institutes of Psychological Sciences, Hangzhou Normal University, Hangzhou, People's Republic of China

³Zhejiang Key Laboratory for Research in Assessment of Cognitive Impairments, Hangzhou, People's Republic of China

⁴Center for Cognition and Brain Disorders, The Affiliated Hospital of Hangzhou Normal University, Hangzhou, People's Republic of China

Correspondence

Jue Wang, Institute of Sports Medicine and Health, Chengdu Sport University, Chengdu 610041, Sichuan, People's Republic of China. Email: juefirst@cdsu.edu.cn

Funding information

Department of Science and Technology of Sichuan Province, Grant/Award Number: 2022NSFSC0808; National Natural Science Foundation of China, Grant/Award Number: 81701776

Abstract

Repetitive transcranial magnetic stimulation (rTMS) has been used in the clinical treatment of Parkinson's disease (PD). Most of rTMS studies on PD used high-frequency stimulation; however, excessive nonvoluntary movement may represent abnormally cortical excitability, which is likely to be suppressed by low-frequency rTMS. Decreased neural activity in the basal ganglia on functional magnetic resonance imaging (fMRI) is a characteristic of PD. In the present study, we found that low-frequency (1 Hz) rTMS targeting individual finger-tapping activation elevated the amplitude of local neural activity (percentage amplitude fluctuation, PerAF) in the putamen as well as the functional connectivity (FC) of the stimulation target and basal ganglia in healthy participants. These results provide evidence for our hypothesis that low-frequency rTMS over the individual task activation site can modulate deep brain functions, and that FC might serve as a bridge transmitting the impact of rTMS to the deep brain regions. It suggested that a precisely localized individual task activation site can act as a target for low-frequency rTMS when it is used as a therapeutic tool for PD.

KEYWORDS

local neural activity, low-frequency rTMS, modulatory effect, putamen, task activation

1 | INTRODUCTION

Repetitive transcranial magnetic stimulation (rTMS) causes long-lasting effects and can be used to modulate brain activity by altering the electrophysiological properties of cortical areas (Pascual-Leone et al., 2005). rTMS may enhance or suppress cortical excitability depending on the stimulation parameters and paradigms (Pascual-Leone et al., 1998). However, the effective range of a TMS figure-8

coil is restricted on the cortical surface to a depth of 2–4 cm. This poses a challenge when the ideal stimulation sites are deeper than 4 cm.

Functional connectivity (FC) of functional magnetic resonance imaging (fMRI) reflects the relationships between brain regions (Biswal et al., 1995; Fox et al., 2005; Friston et al., 1993). Several studies reported that stimulating on superficial target can impact the neuroactivity of the deep brain structure which is functionally connected with the superficial target (Cash et al., 2020; Feng et al., 2021; Wang et al., 2014, 2020). When rTMS is delivered at the parietal lobe it can

Jue Wang and Xin-Ping Deng contributed equally to this study.

This is an open access article under the terms of the [Creative Commons Attribution-NonCommercial](https://creativecommons.org/licenses/by-nc/4.0/) License, which permits use, distribution and reproduction in any medium, provided the original work is properly cited and is not used for commercial purposes.

© 2022 The Authors. *Human Brain Mapping* published by Wiley Periodicals LLC.

induce increased hippocampal FC and enhance the performance of memory (Wang et al., 2014). The brain network identified by FC may act as a “bridge” to transmit the impact of rTMS to the hippocampus to enhance its function and further improve memory performance. These studies suggested that the neuroactivity of deep brain regions can be indirectly modulated by rTMS through the network identified by FC. However, FC only reflects the relationship between the stimulation target and the hippocampus, and alterations in FC alone cannot indicate whether the stimulation target or hippocampus was changed. Percentage amplitude fluctuation (PerAF) is a metric based on voxel-wise spontaneous BOLD activity (Jia et al., 2020; Zhao et al., 2018), and is derived from the more well-known local brain activity metric of amplitude of low-frequency fluctuation (ALFF), and has higher reliability. PerAF can measure whether the neuroactivity of the deep/effective region is modulated by rTMS (Feng et al., 2021).

The putamen, together with the caudate, forms the dorsal striatum, a part of the basal ganglia belonging to the cortico-striato-thalamo-cortical (CSTC) network. This network receives convergent excitatory afferents from the cortex and thalamus (Middleton & Strick, 2000; Mink, 2006), and the putamen receives topographic projections from the primary motor area (Alexander & Crutcher, 1990). Studies in human patients with PD have found decreased activity in the putamen, indicating that it plays a pivotal role in motor function (Herz et al., 2014; Playford et al., 1992; Wang et al., 2018). Some studies observed decreases in FC between the premotor cortex and the putamen in patients with PD in the “OFF” state (Esposito et al., 2013; Wu et al., 2009). Thus, the lateral motor area seems to be the ideal stimulation target for modulating the function of the putamen.

Patients with PD show impaired performance in certain tasks involving timing control or temporal perception, with this being caused by dysfunctions in the basal ganglia (O'Boyle et al., 1996). The basal ganglia are especially involved in the self-initiated execution of movement (Francois-Brosseau et al., 2009). Self-paced and externally cued motor control involve in separate cortico-basal ganglia networks (Bichsel et al., 2018; Taniwaki et al., 2006), and only self-initiated movements activated the basal ganglia (Cunnington et al., 2002). Our previous study has found that fMRI finger-tapping activation in the premotor cortex could as an rTMS target to induce a better modulatory effect on motor-related brain regions including the basal ganglia. We postulate that this is due to more intense FC compared with the hand motor hotspot (Wang et al., 2019). Additionally, there is evidence that FC strength can predict the rTMS modulatory effect (Cash et al., 2020; Feng et al., 2021). However, we could not observe the network differences in voxel-wise FC when using the peak activation voxel of two types of finger-tapping tasks in basal ganglia as seeds within the same session of resting-state fMRI. Thus, we designed a new fMRI paradigm that we named “Steady-state” to magnify the differences and improve their observation. After we observed stronger FC in the “self-initiated state” data, the self-initiated task was selected to generate the peak activation voxel in the contralateral motor cortex to act as a stimulation target for guiding rTMS to modulate the basal ganglia function. The Steady-state sessions used a fixed-interval

event-related design and participants were asked to continuously perform a finger-tapping task every 2 s. Both self-initiated and visual-guided finger-tapping Steady-state scanning sessions were lasted for 8 min.

Both 1 and 10 Hz rTMS have been used in the previous studies on PD (Elahi et al., 2009; Lefaucheur et al., 2014). Therefore, we applied both 1 and 10 Hz rTMS, as well as sham stimulation, to the individual finger-tapping peak activation voxel, to examine modulatory effects on the deep brain region (basal ganglia) in healthy participants. We hypothesized that rTMS delivered to the individual precisely localized target (self-initiated finger-tapping peak activation voxel) would modulate the local neural activity of the basal ganglia via the network identified by FC, regardless of whether the FC was altered or not.

2 | MATERIALS AND METHODS

2.1 | Overall experiment design

The experiment included two sections. It was a within-subject design with each section. Section 1 aimed to select an appropriate finger-tapping task, whereas the purpose of Section 2 was to stimulate the site of the fMRI task activation for modulatory purposes. Participants in both sections underwent MRI scanning consisting of a structural MRI acquisition and two fMRI sessions: a resting-state fMRI (RS-fMRI) acquisition and a finger-tapping task fMRI acquisition. In addition, participants also underwent fMRI scanning for a self-initiated state and a visual-guided state for Section 1 and participated in three rTMS sessions (10 Hz, 1 Hz, and sham) on three separate days for Section 2. The stimulation sessions were randomly arranged across participants and were performed at least 1 week apart. For each rTMS session, all participants underwent pre- and post-rTMS MRI scanning. Both the pre- and post-rTMS scanning consisted of RS-fMRI and task fMRI. The interval between the end of pre-rTMS scanning and the beginning of the rTMS session was kept consistent with that of the first day (1–2 h). The post-rTMS scanning was started as quickly as possible after the rTMS (<30 min). The overall experimental design is shown in Figure 1.

2.2 | Participants

For Section 1, we recruited 42 healthy, right-handed adults (aged 18–48 years, 22 women, mean age 24 years \pm 5.0 [SD]), while for Section 2 we recruited 33 healthy right-handed adults (aged 19–30 years, 23 women, mean age 23 years \pm 2.8). All participants had normal or corrected to normal visual acuity, no history of neurological or psychiatric disease, and gave informed written consent prior to participation (NCT03497884). This study was approved by the ethics committee of the Center for Cognition and Brain Disorders, Hangzhou Normal University. Two participants were excluded from Section 2: one because of head motion exceeding 2 mm in translation or 2° in rotation, and one because of a lack of activation in the task fMRI.

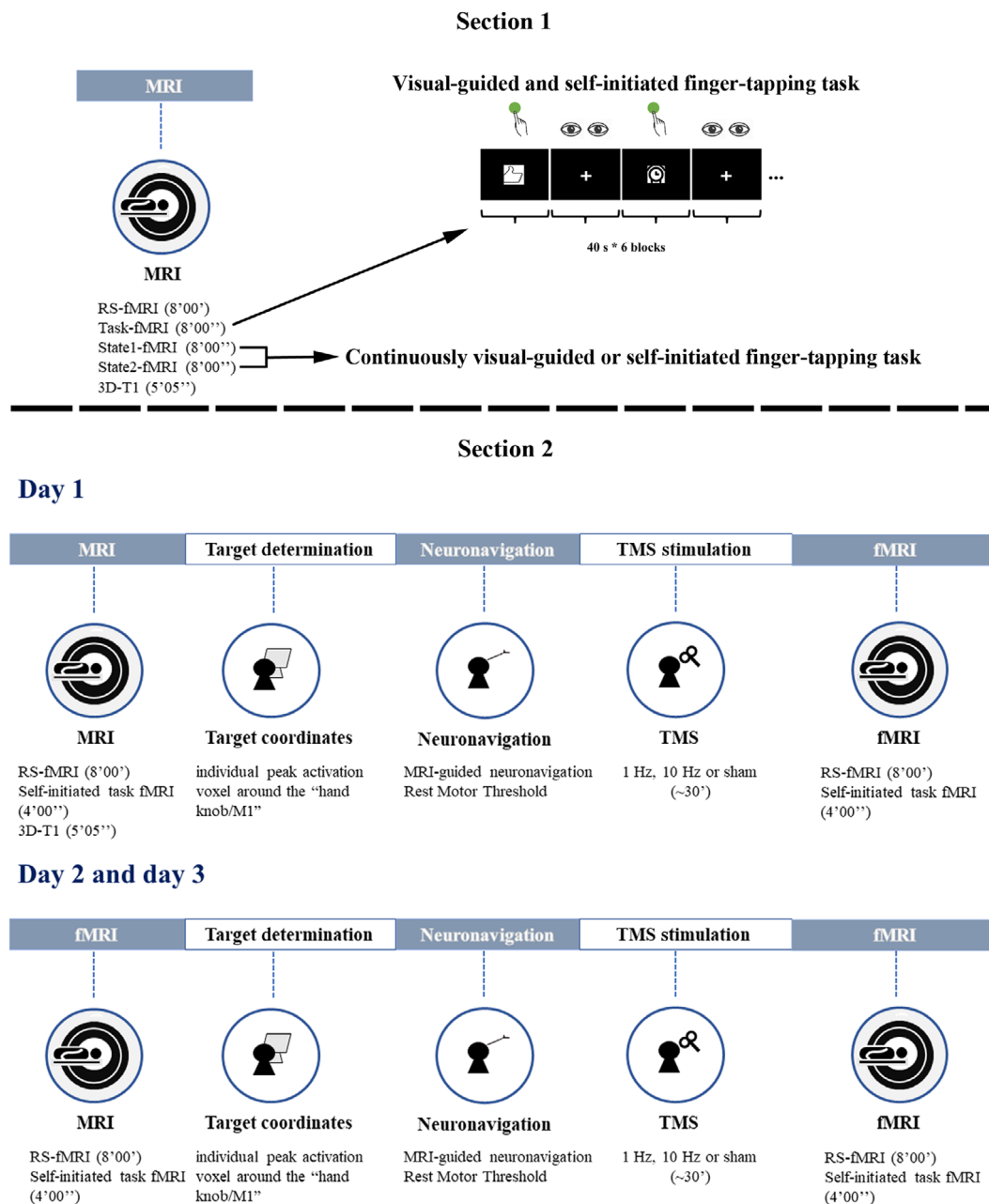


FIGURE 1 A schematic of the experiment protocol. fMRI, functional magnetic resonance imaging; RS-fMRI, resting-state fMRI; TMS, transcranial magnetic stimulation

After carefully checking, all 42 participants were included in the final analysis of Section 1, and 31 participants were included in the final analysis of Section 2. Seven participants participated in both sections.

2.3 | MRI data acquisition

The acquired MRI data included RS-fMRI data sets, pre- and post-rTMS task-fMRI data sets, and pre-rTMS T1 images. The T1 images acquired on the first day were taken to the data analysis for co-registered to the fMRI images. The RS-fMRI session lasted for 8 min,

during which participants were instructed to keep their eyes closed, not to think of anything, and remaining motionless. The task fMRI session used a block design. In Section 1, the task design contained three kinds of blocks (duration 40 s) and lasted for 8 min. In the visual-guided block, participants were required to press a button as quickly as possible with the right index finger when a picture of a finger appeared in the center of the screen. In the self-initiated block, participants were required to press the button at a self-paced interval of every 2 s when a picture of a clock appeared in the center of the screen. For the rest blocks, participants were asked to relax with their eyes fixed on a cross in the center of the screen (Figure 1). The

TABLE 1 The group-level activation differences between self-initiated and visual-guided task

Brain region	Brodmann area	Montreal neurological institute (X Y Z)			Cluster size (mm ³)	T	Q
Left middle occipital lobe	17	-9	-105	3	26,703	6.19	<0.05
Right Cerebellum_8		27	-66	-57	6750	5.12	<0.05
Left middle occipital lobe	19	-42	-72	33	18,414	-6.16	<0.05
Left cuneus	18	-3	-78	24	108,594	-7.55	<0.05
Left supplementary motor area (extend to bilateral pre- and post-central gyrus, bilateral frontal gyrus, bilateral basal ganglia and insula, bilateral hippocampus)	6	-3	0	66	298,161	8.79	<0.05
Left medial frontal gyrus	11	-3	48	-15	5292	-4.34	<0.05
Left superior frontal gyrus	9	-12	51	42	7695	-4.60	<0.05
Right superior frontal gyrus	9	21	39	45	3807	-4.64	<0.05

Note: Q value, FDR correction.

Abbreviation: FDR, false discovery rate.

Steady-state (self-initiated state and the visual-guided state) data were acquired only in Section 1. Only the self-initiated task was employed in Section 2 (block duration 30 s), where it lasted for 4 min.

Participants underwent MRI scanning on a GE Discovery MR-750 3.0-T scanner (GE Medical Systems) at the Center for Cognition and Brain Disorders of Hangzhou Normal University. The participant's head was snugly fixed by foam pads to minimize head movement and ear-plugs were used to reduce noise while the participant lay supine in the scanner. A 3D T1-weighted image for co-registration was acquired for each participant using a spoiled gradient-recalled pulse sequence (176 sagittal slices, thickness = 1 mm, repetition time [TR] = 8.1 ms, echo time [TE] = 3.1 ms, flip angle = 8°, field of view [FOV] = 250 × 250 mm²). Functional images were acquired using a gradient-echo echo-planar sequence sensitive to blood oxygen level-dependent (BOLD) contrast (TR = 2000 ms, TE = 30 ms, flip angle = 90°, FOV = 24 × 24 cm², matrix = 64 × 64). Forty-three 3.2-mm-thick axial slices with no between slice gap were collected. The in-plane resolution was 3.44 × 3.44 mm. The scanner room was kept dim during scanning.

2.4 | Section 1: MRI data analysis for selecting the finger-tapping task

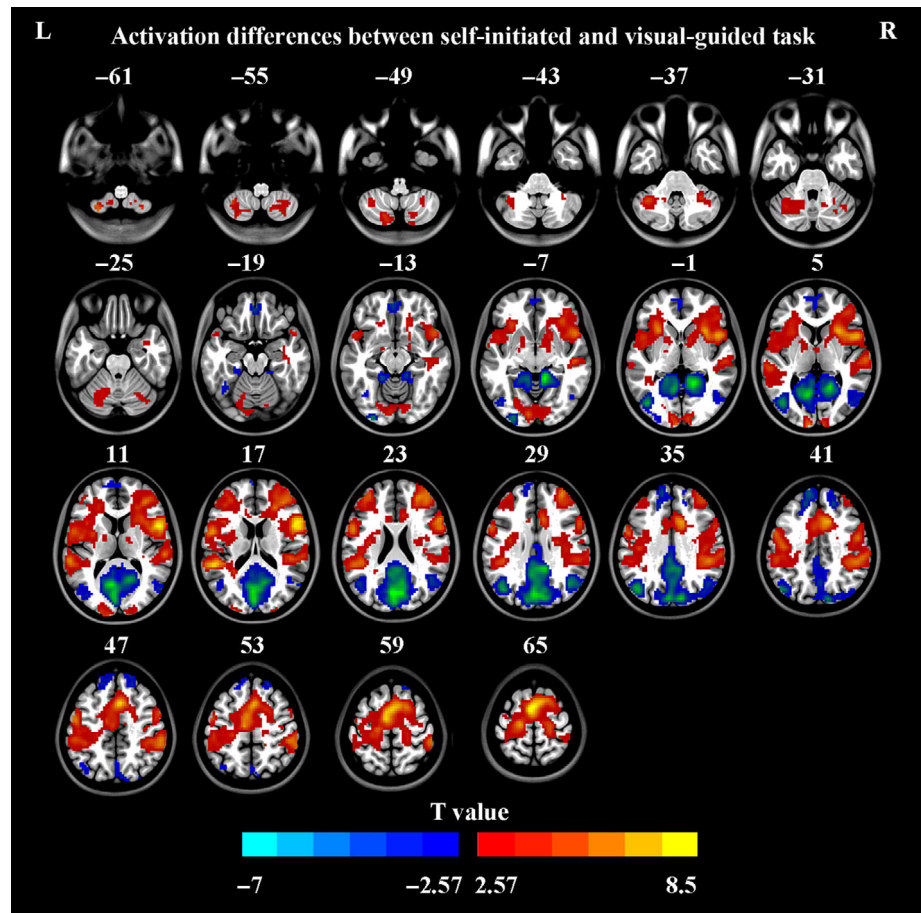
Preprocessing of the task-fMRI data acquired for Section 1 was performed using the data processing assistant for resting-state fMRI (DPARF, <http://rfmri.org/DPABI>). The preprocessing steps were: (1) slice timing correction, (2) head motion correction, (3) nonlinear registration of the high-resolution T1 structural images to the Montreal Neurological Institute (MNI) template and segmentation into white matter, gray matter, and CSF using the New segment algorithm, (4) normalization of functional images to MNI space using the transformation matrix obtained from T1 segmentation and normalization followed by resampling to a spatial resolution of 3 × 3 × 3 mm³; (5) spatial smoothing with a Gaussian kernel (full width at half-maximum = 6 × 6 × 6 mm³).

Following the preprocessing, the subject-level activation analysis was conducted using Statistical Parametric Mapping 12 software (SPM12, <https://www.fil.ion.ucl.ac.uk/spm/software/spm12/>) to generate subject-level activation maps.

The group-level activation map for Section 1 was generated in SPM12 (Table 1 and Figure 2, FDR correction, $q < 0.05$). The self-initiated task showed higher activation in motor-related brain regions than the visual-guided task, with these brain regions including the cerebellum VIII area, supplementary motor area (SMA), pre- and post-central gyrus, and basal ganglia. Some other regions related to more-cognitive elements of movement also showed higher activation in the self-initiated task than in the visual-guided task, with these regions including the frontal gyrus, insula, and hippocampus. Therefore, a basal ganglia mask was created from the Anatomical Automatic Labeling (AAL) template (Tzourio-Mazoyer et al., 2002) (Figure 3) and the individual self-initiated and visual-guided task peak activation voxels within the region defined by basal ganglia mask (Table S1) were used as the seeds for the following FC analysis.

Preprocessing of both RS-fMRI and Steady-state fMRI data were also performed using DPARF. The preprocessing steps were: (1) removal of the first 10 time points to avoid transient signal changes and to allow participants to adapt to the fMRI scanning environment; (2) slice timing correction; (3) head motion correction; (4) co-registration of functional images to T1 images; (5) nonlinear registration of high-resolution T1 structural images to the Montreal Neurological Institute (MNI) template and segmentation into white matter, gray matter, and cerebrospinal fluid (CSF) using the DARTEL segment algorithm (Ashburner, 2007); (6) removal of nuisance signal (white matter, CSF, head motion [Friston 24-parameters]) (Friston et al., 1996; Yan et al., 2013, 2016) and polynomial trends through multiple regression; (7) bandpass filtering (0.01–0.08 Hz); (8) normalization of functional images to MNI space using the transformation matrix obtained from the T1 segmentation and normalization, then resampling to a spatial resolution of 3 × 3 × 3 mm³; (9) spatial smoothing with a Gaussian kernel (full width at half-maximum = 6 × 6 × 6 mm³).

FIGURE 2 Group-level finger-tapping task activation differences between the self-initiated and visual-guided task (FDR correction, $q < 0.05$). The warm color indicates that self-initiated activation is higher than visual-guided activation. FDR, false discovery rate



Basal ganglia (BG) mask

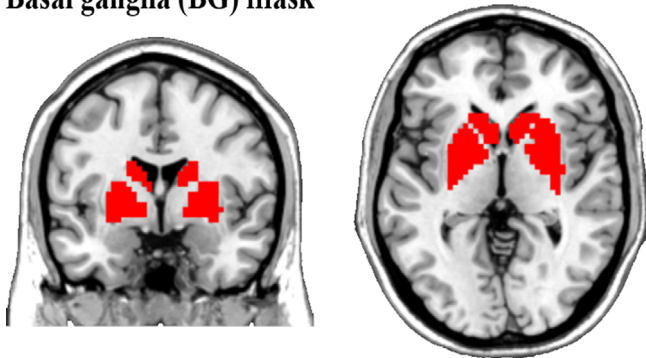


FIGURE 3 The basal ganglia mask from the AAL template. AAL, anatomical automatic labeling

Thus, the individual self-initiated and visual-guided task peak activation voxels (Table S1) within the basal ganglia mask were taken as the seeds (peak voxel as the center of a 4-mm-radius sphere [7 voxels]) for the voxel-wise FC analysis using the DPARSF toolkit, which was performed on both the RS-fMRI data and Steady-state data. The RS-fMRI data did not show a significant difference between self-initiated-based and visual-guided-based FC. The self-initiated state data showed significantly higher FC than the visual-guided state (Figure 4, GRF [Gaussian Random Field] correction, single voxel $p < .001$, cluster

level $p < .05$). Ultimately, the self-initiated task was selected to guide the navigated rTMS.

2.5 | Section 2: fMRI-guided navigated rTMS

2.5.1 | MRI data analysis for defining the target

The self-initiated task fMRI data and T1 image were analyzed in SPM12 in the original acquisition space to identify the individualized rTMS targets after the following preprocessing steps: (1) slice timing correction, (2) head motion correction, (3) co-registration of functional images to T1 image, and (4) spatial smoothing with a Gaussian kernel (full width at half-maximum = $6 \times 6 \times 6 \text{ mm}^3$). Then, the individual peak activation voxel around the anatomical landmark formation “hand knob/M1” (Yousry et al., 1997) was identified as the individualized rTMS target for each participant.

2.5.2 | Navigated rTMS

The rTMS was delivered with a 70-mm figure-8 coil (Magstim Rapid² stimulator, Magstim Company) equipped with a frameless stereotactic optical tracking neuronavigation system (Brainsight; Rogue Research)

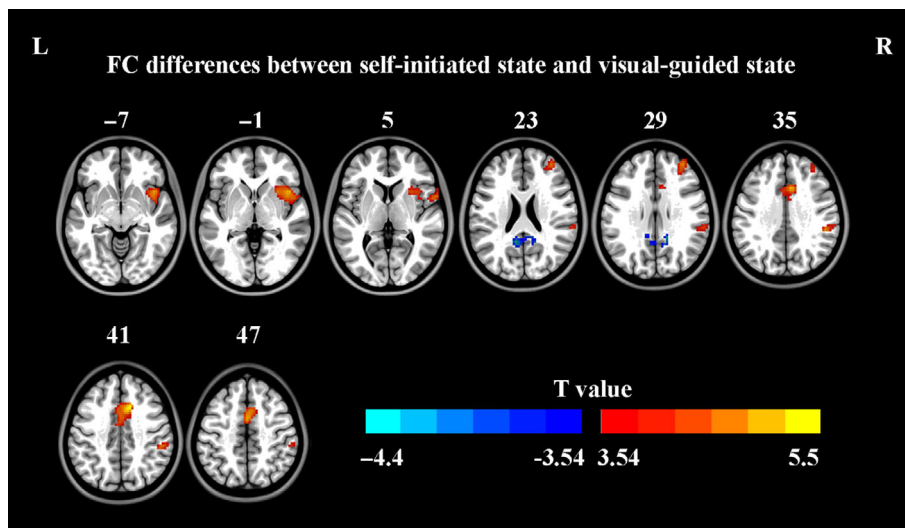


FIGURE 4 The FC differences between self-initiated and visual-guided state (GRF correction, single voxel $p < .001$, cluster $p < .05$). The warm color indicates the FC of self-initiated basal ganglia activation is more intense than that of visual-guided activation. FC, functional connectivity; GRF, Gaussian random field

focused on the activation peak. The position of the coil was tracked and recorded simultaneously by the neuronavigation system during stimulation. To measure the resting motor threshold (RMT), the motor-evoked potentials (MEP) amplitudes of the right first dorsal interosseous (FDI) muscle were recorded using Ag/AgCl surface electromyogram (EMG) leads when stimulating the left “hotspot.” The hotspot was defined as the location where the lowest intensity evoked the highest amplitude MEPs. Participants sat in a comfortable chair with both arms relaxed on their thighs. Full muscle relaxation was confirmed through visual observation and EMG monitoring. TMS started with a subthreshold intensity (35% of the maximal stimulator output) with the coil placed 45° toward the contralateral forehead over the M1 area (Opitz et al., 2013; Rossini et al., 2015). The stimulus intensity was then gradually increased in steps of 5% of the maximal stimulator output. When MEPs were consistently evoked with peak-to-peak amplitudes of $>50 \mu\text{V}$ in each trial, the stimulus intensity was gradually lowered in steps of 1% of the maximal stimulator output. The RMT was quantified as the lowest stimulator output intensity that evoked a response ($>50 \mu\text{V}$) in more than 5 out of 10 consecutive trials plus 1 (Rossini et al., 2015). The actual stimulation intensity was around half of the level of the intensity of the rTMS (mean $58 \pm 6\%$ SD of maximum stimulator output).

The coil was positioned tangentially on the scalp over the target (finger-tapping task activation) to the scalp with the handle pointing posteriorly at 45° to the sagittal plane. The total stimulation of 1800 pulses (100% RMT intensity, duration 30 min) for each stimulation day were designed in accordance with a previous rTMS study (Eldaief et al., 2011). For the low-frequency (1 Hz) session, pulses were delivered continuously for 1800 s. For the high-frequency (10 Hz) session, to keep the session length equal to the low-frequency session, pulses were delivered with 60 trains of stimulation, each lasting 3 s, with rest intervals of 27 s in between (1800 pulses in total). For the sham session, the coil was tilted at 90° to the scalp with one wing touching the scalp (Lisanby et al., 2001). The sham stimulation was randomly assigned so that 1 Hz was used for one half of the participants and 10 Hz for the other half.

2.5.3 | Post-rTMS MRI data preprocessing

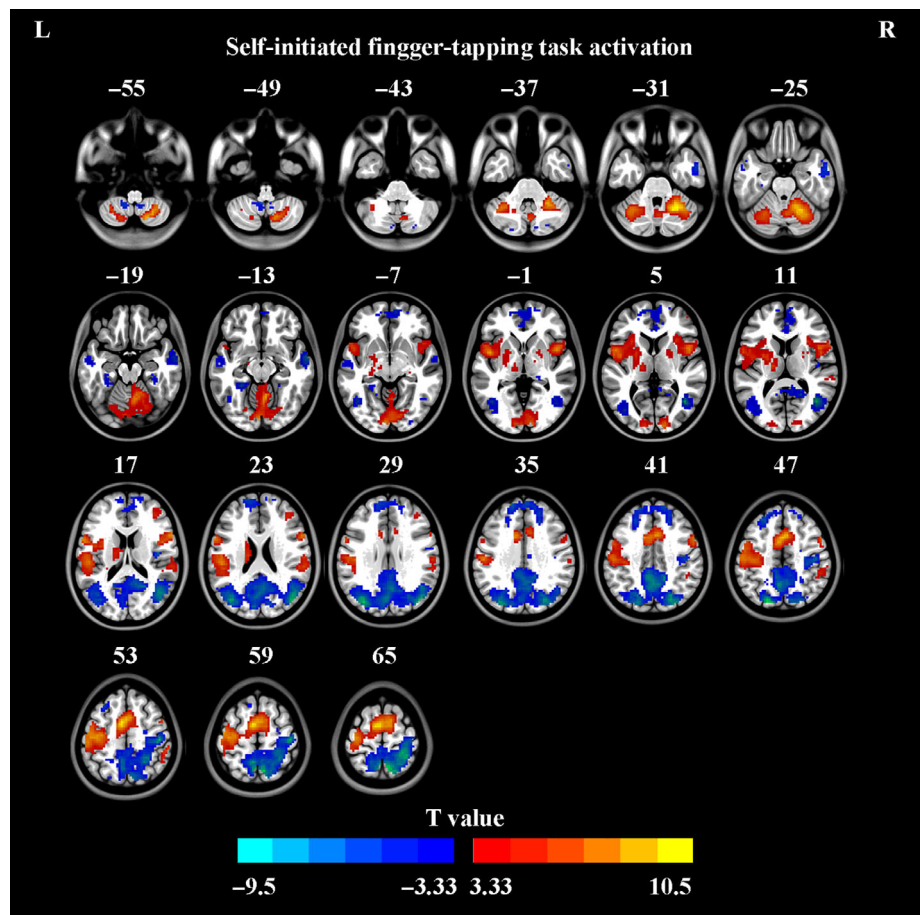
Preprocessing of task and RS-fMRI was also performed using the DPARSF toolkit. The preprocessing steps were the same as described in Section 2.4 “Section 1: MRI data analysis for selecting the finger-tapping task.”

2.5.4 | Post-rTMS MRI statistical analysis

Group-level self-initiated task activation maps were created in SPM12 (Figure 5, FDR correction, $q < 0.05$).

Two metrics, PerAF and FC, were employed to explore the modulatory effects of rTMS on remote brain regions. PerAF was calculated using the Resting-State fMRI Data Analysis Toolkit (RESTplus) (Jia et al., 2019). For the PerAF alteration (post- vs. pre-rTMS), one-way repeated-measures analysis of variance (ANOVA) among the three stimulation conditions (1 Hz, 10 Hz, and sham) was conducted for the whole brain. Multiple comparison corrections were performed within the whole brain (GRF correction, single voxel $p < .001$, cluster level $p < .05$). Then, post-hoc paired t -tests on PerAF maps were performed. For the voxel-wise and ROI-wise FC, two regions of interest (ROIs) were defined: target seed ROIs (self-initiated task activation) and basal ganglia ROIs (basal ganglia mask). Then the voxel-wise FC of the individual-target-seed (a 4-mm-radius sphere) and the mean-target-seed (mean coordinate of all participants' targets as a seed, a sphere of 10-mm radius centered on $X = -45$, $Y = -10$, $Z = 53$) were calculated on the RS-fMRI data separately. The ROI-wise FCs between the target-seed ROIs (individual-target-seed, mean-target-seed) and the basal ganglia ROI were also measured on the RS-fMRI data separately. Paired t -tests were performed to detect the 1 Hz rTMS modulatory effect on voxel-wise FC (post- vs. pre-rTMS; Figure 6; GRF correction, single voxel $p < .001$, cluster level $p < .05$). ROI-wise FC paired t -tests on 1 Hz rTMS modulatory effect (post- vs. pre-rTMS) were conducted in SPSS (SPSS v25.0, IBM Corp.).

FIGURE 5 Group level self-initiated finger-tapping task activation in the whole brain (FDR correction, $q < 0.05$). FDR, false discovery rate



3 | RESULTS

3.1 | Selection of self-initiated finger-tapping task

The self-initiated task showed higher activation in the basal ganglia and stronger activation-based FC in motor-related brain regions than the visual-guided task (Table 1 and Figures 2 and 4).

3.2 | The modulatory effect of rTMS

The locations of activation (stimulation target) varied greatly between individuals. The mean and standard deviation of the MNI coordinates were $X = -45 \pm 7.63$, $Y = -10 \pm 7.99$, $Z = 53 \pm 5.99$. The spatial distribution was mapped by using the BrainNet Viewer toolkit (Xia et al., 2013) (Figure 7). The group-level activation map showed extensive activation from the self-initiated finger-tapping task throughout the whole brain (Figure 5). No significant task activation alteration was observed among all three rTMS sessions (post- vs. pre-rTMS).

The whole brain ANOVA on PerAF showed significant differences among the stimulation conditions (1 Hz, 10 Hz, and Sham) in the whole brain including basal ganglia (Figure 8). Post-hoc paired *t*-tests showed significantly increased higher PerAF in the left putamen

following the 1 Hz rTMS intervention ($X = -21$, $Y = 9$, $Z = 0$; $t = 7.17$, GRF correction within the whole brain, single voxel $p < .001$, cluster $p < .05$) (Figures 9 and 10a) and further analysis revealed that this alteration was mainly concerned the slow-4 frequency band (0.027–0.073 Hz; the results of slow-4 were corrected for the basal ganglia volume using a small volume GRF correction, single voxel $p < .001$, cluster $p < .05$; Figure 10a). The slow-4 band in the low-frequency oscillations were most robust in the basal ganglia, and have also been found in spontaneous electrophysiological recordings in the awake rat (Buzsaki & Draguhn, 2004). A human resting-state fMRI study also observed the slow-4 band in the basal ganglia with good test–retest reliability (Zuo et al., 2010).

The significant mean-target-seed ($X = -45$, $Y = -10$, $Z = 53$) voxel-wise FC alterations were found in the bilateral basal ganglia, right cerebellum, and brainstem (Table 2 and Figure 6). The ROI-wise FCs between the mean-target and the basal ganglia were also significantly altered following 1 Hz rTMS ($t = 4.194$, $p = .0002$), as well as those between mean-target and the left putamen (a 4-mm-radius sphere centered on a significant PerAF alteration peak, 7 voxels; $t = 2.691$, $p = .012$).

The 10 Hz rTMS stimulation induced significant increases in regional homogeneity (ReHo) in the contralateral cerebellum VIII area extending to the VIIIb area, as found in our prior work (Wang et al., 2020).

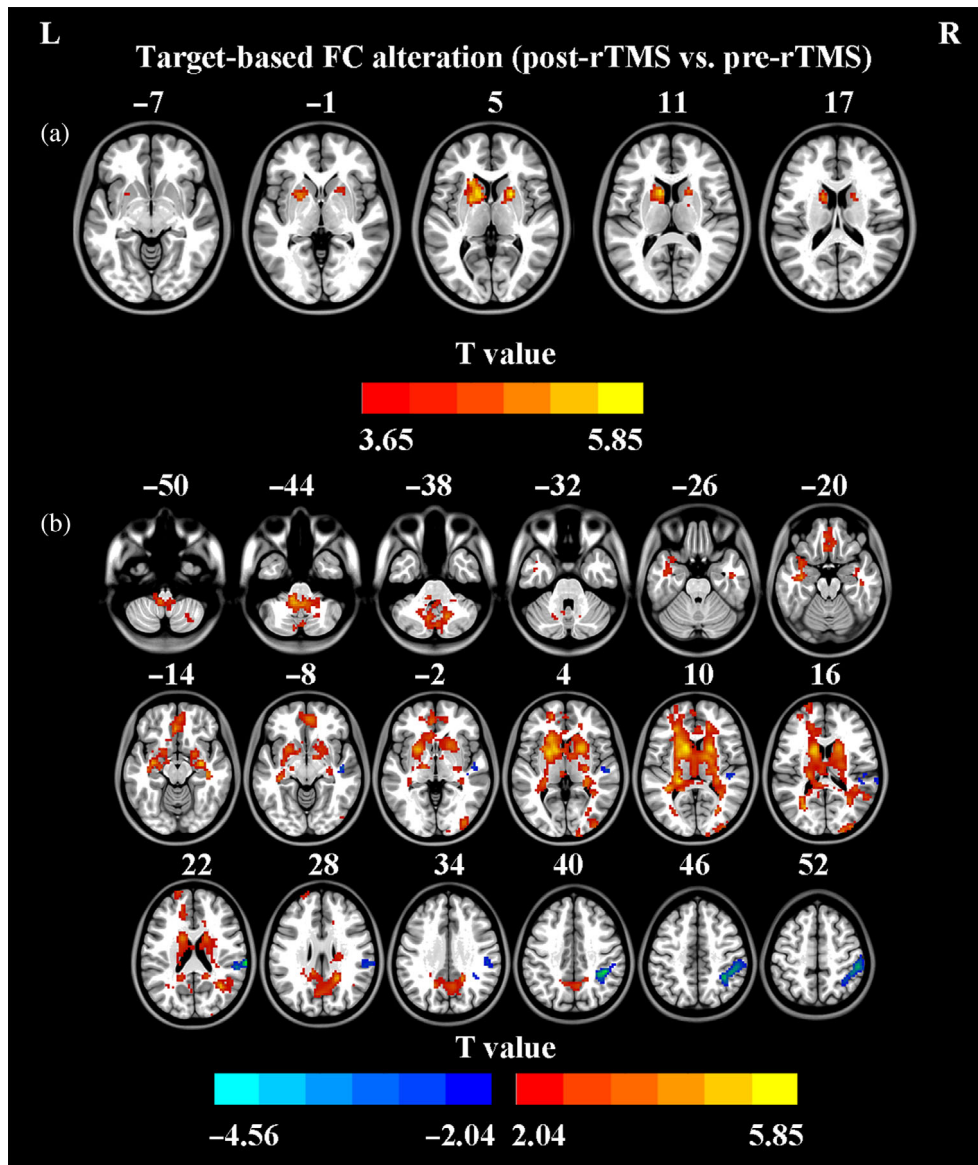


FIGURE 6 The mean-target-based FC alteration following 1 Hz rTMS (post- vs. pre-rTMS). (a) Multiple comparison correction within the whole brain (GRF correction, single voxel $p < .001$, cluster $p < .05$); (b) multiple comparison correction within the whole brain (GRF correction, single voxel $p < .05$, cluster $p < .05$). The warm color indicates elevated FC. FC, functional connectivity; GRF, Gaussian random field; rTMS, repetitive transcranial magnetic stimulation

4 | DISCUSSION

The present study reveals a modulatory effect of rTMS on local neural activity in the target ipsilateral putamen. We observed alterations in FC between the stimulation target and the putamen, as well as elsewhere in the whole brain. These findings provide evidence to corroborate our hypothesis that the rTMS impact was delivered from the superficial cortex to the deep brain area via networks identified by FC, with low-frequency rTMS targeted to an individual fMRI finger-tapping task activation modulating local neural activity in the putamen.

4.1 | Basal ganglia and motor function

The basal ganglia are highly interconnected subcortical nuclei that provide critical motivation, motor planning, and procedural learning functions (Hikosaka et al., 2000; Nicola, 2007; Packard &

Knowlton, 2002; Yin & Knowlton, 2006). Dysfunction of the basal ganglia is associated with neurological disorders such as PD (McGregor & Nelson, 2019). Certain aberrant neural activities associated with cognitive and behavioral impairments were seen in dysfunctions of the basal ganglia loops (Carriere et al., 2014; Chung et al., 2018; Wang et al., 2017). Despite the importance of basal ganglia in disease-related malfunction, only a limited number of studies have explored the modulatory effects of rTMS on basal ganglia. High-frequency rTMS at 10 Hz targeting the prefrontal cortex was reported to induce the release of endogenous dopamine in the ipsilateral caudate nucleus (Strafella et al., 2001). Additionally, stimulation of the pre-SMA with a quadro-pulse stimulation (1.5 ms intervals repeated every 5 s) was also reported to significantly affect intrinsic FC between the pre-SMA and the striatum (Watanabe et al., 2015). High-frequency (20 Hz) rTMS over the left prefrontal cortex induced significant regional cerebral blood flow (rCBF) elevation in the basal ganglia, while low-frequency (1 Hz) rTMS induced decreased rCBF in the basal

FIGURE 7 The spatial distribution of the individual stimulation targets (red dots). The mean MNI coordinates (\pm SD) of the fMRI activation were $X = -45 \pm 7.63$, $Y = -10 \pm 7.99$, $Z = 53 \pm 5.99$ (green dot). MNI, Montreal Neurological Institute

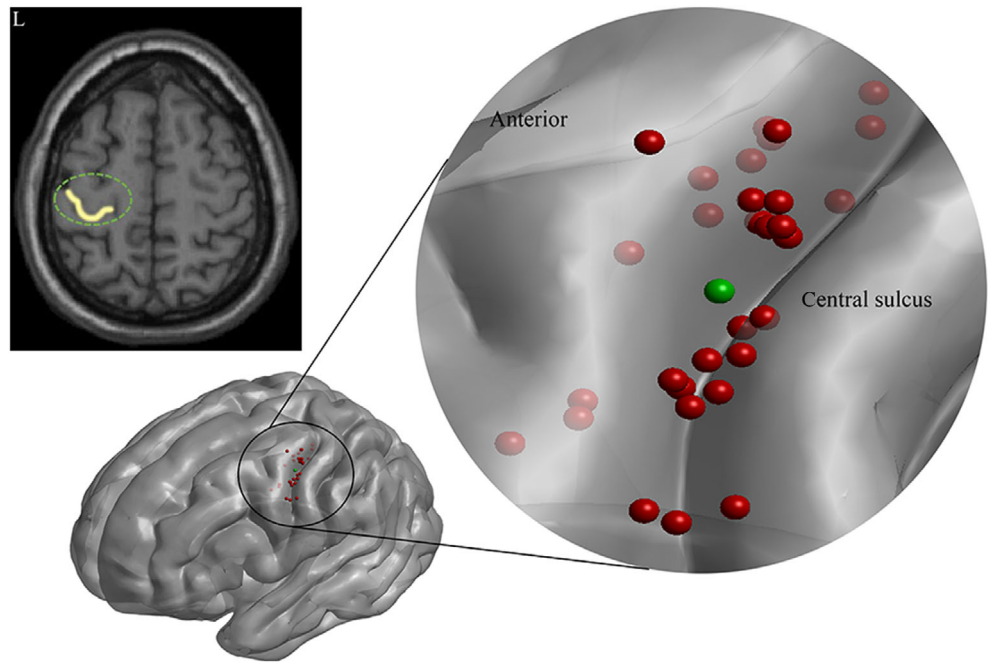
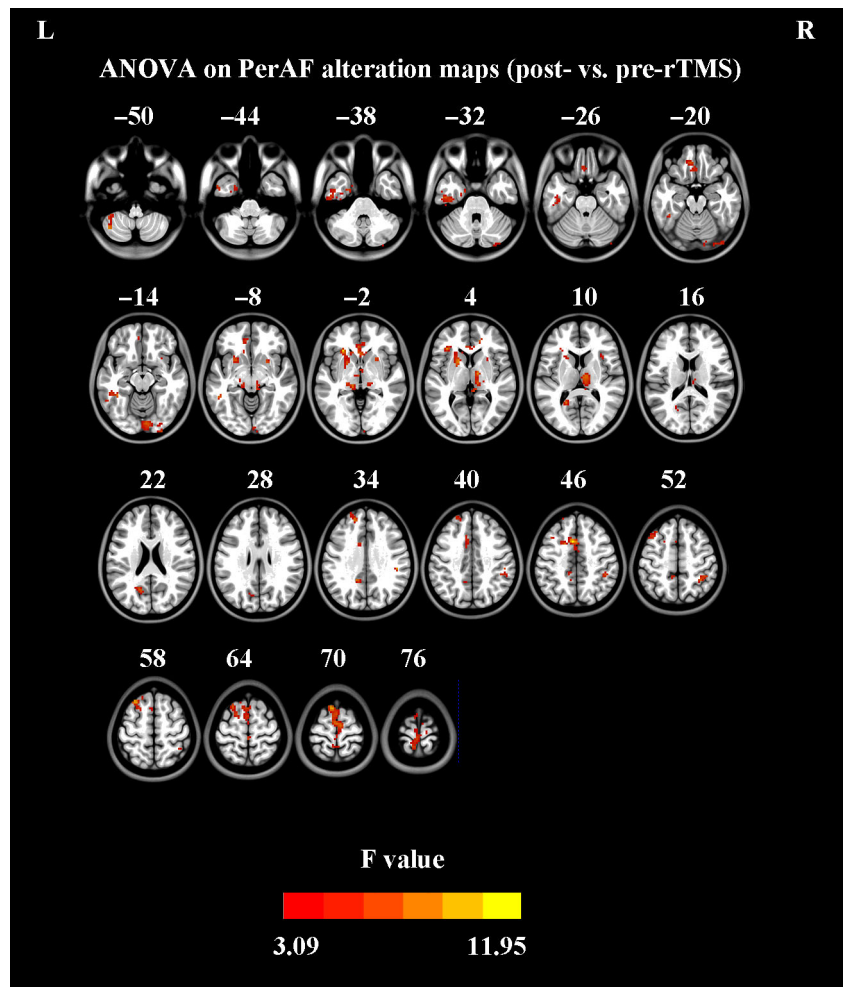


FIGURE 8 ANOVA on PerAF alteration maps (post- vs. pre-rTMS) among three stimulation conditions (1 Hz, 10 Hz, and Sham) (GRF correction, single voxel $p < .001$, cluster $p < .05$). GRF, Gaussian random field; rTMS, repetitive transcranial magnetic stimulation



Alterations of PerAF in the left putamen (post- vs. pre-rTMS)

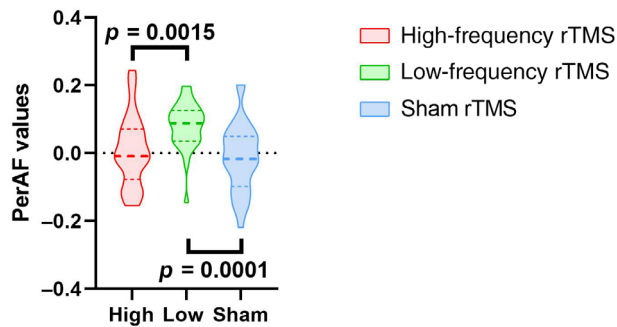


FIGURE 9 Alterations of PerAF in the left putamen among the stimulation conditions (post- vs. pre-rTMS). The 1 Hz rTMS significantly increased PerAF compared with 10 Hz and sham rTMS. rTMS, repetitive transcranial magnetic stimulation

ganglia (Speer et al., 2000). However, which rTMS targets and stimulation protocols exerts modulatory effects on basal ganglia remains unclear.

4.2 | Self-initiated or visual-guided finger-tapping task to navigate rTMS

The basal ganglia are responsible for the impaired performance of patients with PD in a variety of tasks requiring timing control or temporal perception (O'Boyle et al., 1996). A recent deep brain recording study reported that self-paced and externally cued motor execution involved functionally separated networks (Bichsel et al., 2018). We previously found that fMRI activation from finger-tapping gave more intensive FC through the whole brain than the hand motor hotspot, especially for motor-related brain regions including the basal ganglia (Wang et al., 2019). However, we needed to decide which type of finger-tapping task best fitted the purpose of the present study. The current results showed that the self-initiated task produced more activation than the visual-guided task in some motor-related brain regions, including the basal ganglia. The traditional RS-fMRI data acquisition and analysis did not reveal the network differences between the two tasks, with the individual activation peak-based FC extracted from RS-fMRI not detecting any difference. However, the newer "Steady-state" paradigm of finger-tapping did show a difference; the self-initiated finger-tapping was more intensively associated with the motor-related brain regions than visual-guided finger-tapping (Figure 4). As mentioned above, more intensive FC might result in a better modulatory effect; therefore, the self-initiated finger-tapping task was chosen to navigate rTMS.

4.3 | TMS modulatory effect on the basal ganglia

An study showed that cerebral blood flow (CBF) of the caudate in nonhuman primates was robustly activated by high-frequency rTMS

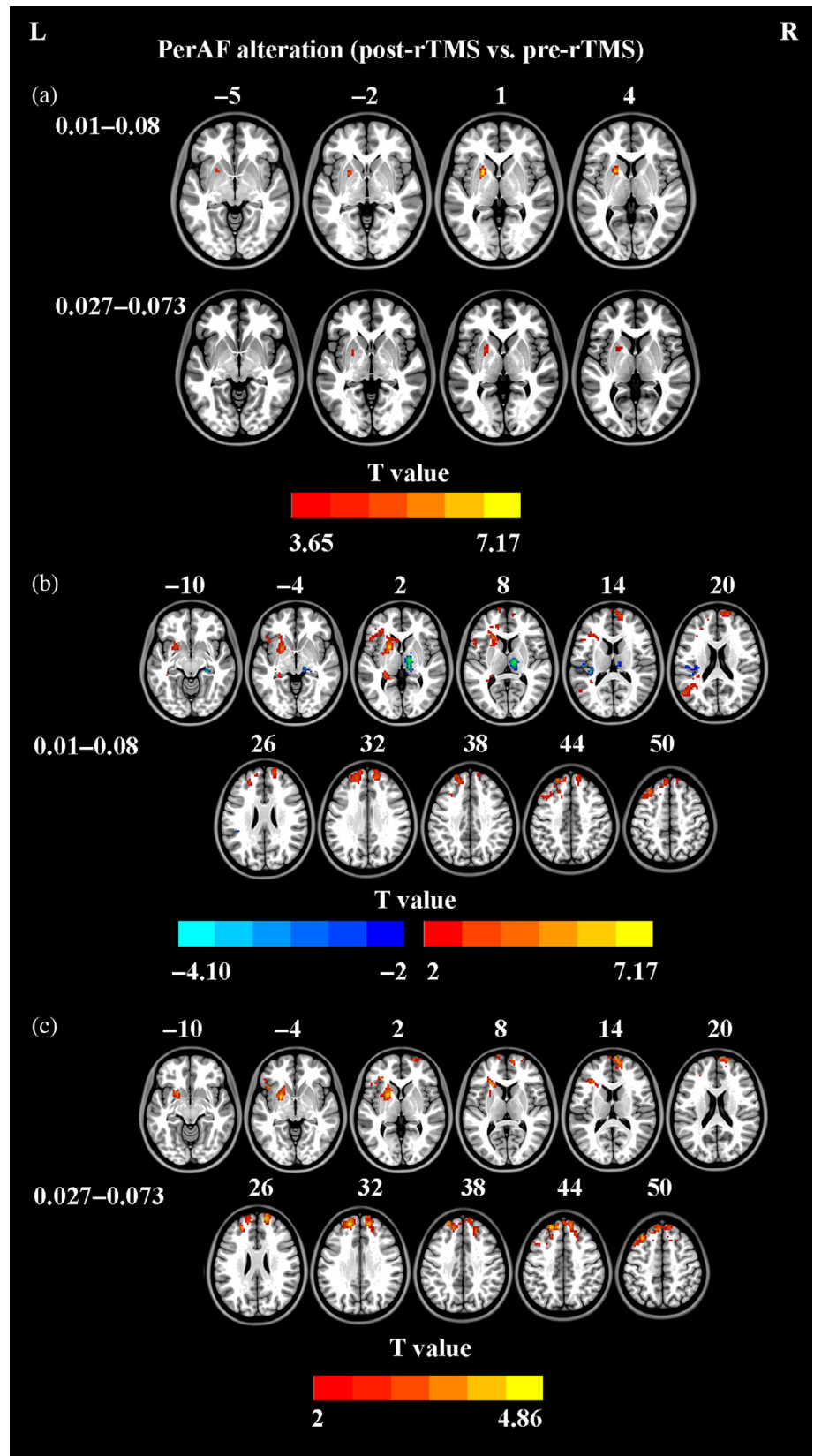
(Salinas et al., 2013). Quantification with a positron emission tomography (PET) study showed further evidence for an rTMS modulatory effect on the putamen, with a release of dopamine was found following 10 Hz rTMS over the medial prefrontal cortex (Cho et al., 2015). Our previous work revealed a decreased amplitude of local neural activity in the left putamen in a large sample of patients with PD (Wang et al., 2018). The present study found that 1 Hz rTMS resulted in significantly increased local neural activity in the left putamen, which is almost the same area affected in the aforementioned PET study mentioned above. Further sub-frequency analysis indicated that the main contribution to these alterations was mainly from the slow-4 band (0.027–0.073 Hz), which is consistent with a previous finding that the local activity of the putamen is sensitive to the slow-4 band (Zuo et al., 2010). Meanwhile, the FC between the putamen and the stimulation target was also significantly enhanced. These findings suggested that the modulatory effect of rTMS might be delivered from the superficial target (finger-tapping activation) to the deep brain area (putamen) via network identified by FC, which might serve as a bridge to transfer the modulatory effect.

Reduced dopamine uptake in the putamen leads to Parkinsonian symptoms (Brooks et al., 1990). Many rTMS studies on the clinical treatment of PD have reported wide variations in targets and stimulation protocols (Elahi et al., 2009; Lefaucheur, 2009; Wu et al., 2008). M1 is the most common rTMS target, although its curative effects are modest (Benninger, 2013), making it difficult to apply in clinical practice. The consensus is that the therapeutic target should be more precise and specific to the disease or symptom. The present study employed finger-tapping activation as the target because of its intensive FC, with a significant increase in the amplitude of the local neural activity of the putamen. Our results may increase the understanding of the neuroimaging mechanism behind the rTMS modulatory effect and potentially support the use of finger-tapping activation for identifying a therapeutic rTMS target for treatment of PD.

4.4 | High- and low-frequency rTMS modulatory effects on different brain functions

It is not certain that high-frequency rTMS induces excitatory effects and low-frequency rTMS induces inhibitory effects. A basic science study on nonhuman primates found that high-frequency (5 Hz) rTMS revealed the strong path coefficients on the nodes of the motor network, but that it did not "excite" all nodes of the motor network, with the specific node-to-node influence depending on the specific brain network (Salinas et al., 2016). Human studies also observed these uncertain modulatory effects, with the effects being highly dependent on the properties of the brain network and the status of the population (Lefaucheur, 2019). In addition to fMRI, TMS-induced local neural activity changes have been investigated with PET, magnetic resonance spectroscopy, and arterial spin-labeling in addition to fMRI (Diekhoff et al., 2011; Vidal-Pineiro et al., 2015). However, the mechanism of the modulatory effect remains unclear. Our former work only observed the synchronization alteration in the cerebellum in high-

FIGURE 10 The PerAF alteration following 1 Hz rTMS (post- vs. pre-rTMS). (a) For the 0.01–0.08 Hz band, multiple comparison correction within the whole brain (GRF correction, single voxel $p < .001$, cluster $p < .05$), for the 0.027–0.073 Hz band, small volume correction within the basal ganglia mask (GRF correction, single voxel $p < .001$, cluster $p < .05$); (b) multiple comparison correction within the whole brain (GRF correction, single voxel $p < .05$, cluster $p < .05$) for the 0.01–0.08 Hz band; (c) multiple comparison correction within the whole brain (GRF correction, single voxel $p < .05$, cluster $p < .05$) for the 0.027–0.073 Hz band. The warm color indicates elevated PerAF. BG, basal ganglia; GRF, Gaussian random field; rTMS, repetitive transcranial magnetic stimulation



frequency rTMS session by using whole-brain-analysis but not in low-frequency stimulation session (Wang et al., 2020). Recent clinical studies reported that high-frequency rTMS targeting the lateral motor

cortex significantly increased local neural activity in the sensorimotor cortex and occipital lobe (Liu et al., 2015), and that targeting of the left dorsolateral prefrontal cortex increased local neural activity in the

TABLE 2 Mean-target-seed FC alteration after 1 Hz rTMS (post- vs. pre-rTMS)

Brain region	Brodman area	Montreal neurological institute (X Y Z)			Cluster size (mm ³)	T	Single voxel p
Right cerebellum VIII		21	-66	-48	25,704	4.49	<.001
Right brainstem (extend to bilateral basal ganglia and cerebellum)		3	-33	-12	52,407	4.70	<.001
Left white matter	48	-33	-27	33	999	-3.30	<.001

Abbreviations: FC, functional connectivity; rTMS, repetitive transcranial magnetic stimulation.

rostral anterior cingulate cortex (Xue et al., 2017). In contrast, one study reported no significant alteration in local neural activity after both 1 Hz rTMS and continuous theta burst stimulation (cTBS) targeting the SMA (Ji et al., 2017). A study on depression suggested that a metric of the amplitude of local neural activity, such as ALFF, was not a sensitive predictor of the rTMS effect (Du et al., 2018). Therefore, the present study adopted a relatively new index, PerAF, which is a measure of the local neural activity, and is a derivative of ALFF that reflects the fluctuation of voxel-wise local BOLD signals with more sensitivity and reliability (Feng et al., 2021; Zhao et al., 2018), and has allowed observation of significant fluctuation alterations in the putamen after 1 Hz rTMS.

High-frequency rTMS was reported to induce a stronger aftereffect and better results than low-frequency rTMS (Elahi et al., 2009). However, only 4 of 11 publications conducted low-frequency rTMS in this review (Elahi et al., 2009), which resulted in the conclusion that low-frequency rTMS had little effect on motor symptoms in PD. A guideline published in 2014 also mentioned only four low-frequency rTMS PD studies out of a total of 17 (Lefaucheur et al., 2014). Most rTMS studies of PD used high-frequency stimulation, possibly because of the notion that high-frequency stimulation could induce a stronger modulatory effect. A recent study reported that the short-interval intracortical facilitation (SICF) (tests cortical facilitation) of the lateral motor cortex was increased in PD OFF and PD ON conditions compared with controls (Saravanamuttu et al., 2021). This result is consistent with the clinical manifestations of PD. It seems that the excessive nonvoluntary movement of PD may be suppressed by low-frequency rTMS, as seen when it is applied in patients with tic disorders. Thus, we considered that low-frequency rTMS might be a better stimulation protocol for the treatment of PD.

Our prior work observed an increase in local synchronization in the cerebellum by using regional homogeneity (ReHo) measurement following 10 Hz rTMS (Wang et al., 2020), and in the present study we found an increased amplitude of low-frequency fluctuation in the putamen using PerAF measurement following 1 Hz rTMS. Recently, some studies reported that 1 Hz rTMS showed better modulatory effects than 10 Hz rTMS in patients with PD. A cross-over design for comparing 1 and 10 Hz rTMS found that the 1 Hz stimulation produced a significant modulatory effect (Brabenec et al., 2019). Another study found that both 1 and 10 Hz rTMS showed clinical efficacy with no significant difference between them (Li et al., 2015). The 10 Hz rTMS may have a more beneficial effect on the freezing of gait of patients with PD (Kim et al., 2015;

Lee et al., 2014; Ma et al., 2019; Mi et al., 2019), while 1 Hz rTMS improved self-assessment scores for tremor compared with 20 Hz rTMS (Khedr et al., 2019). These results suggested that the 1 and 10 Hz rTMS induced different modulatory effects (Lefaucheur et al., 2004). Although the relationship between the low-frequency band of fMRI and low-frequency rTMS is still unclear, and the impact of low-frequency rTMS might be weak, current research is “opening perspectives for the therapeutic use of rTMS” (Lefaucheur, 2019). The rTMS-induced alteration of excitability direction may vary widely according to the location of the stimulation target (lateral motor area vs. other brain areas) and the activity level of the recruited brain network (Lefaucheur, 2019). High- and low-frequency rTMS may impact different brain regions and functions in different ways. Future studies should include multi-session rTMS to reinforce and prolong the rTMS modulatory effect and reveal its mode-of-action. Without doubt, further investigations should attempt to involve the clinical populations for validation.

5 | LIMITATIONS

This study is subject to a number of limitations that should be addressed. The local neuroactivity measurements (such as PerAF) and FC were only indirectly measured the remote modulatory effect of rTMS, and the measurements could not be directly associated with cortical excitability. We did not consider the impact of coil direction when we designed the experiment; several studies have focused on precisely positioning and orienting of the rTMS coil by measuring the TMS-induced electric field (E-field) (Arabkheradmand et al., 2019; Fox et al., 2004; Krieg et al., 2013, 2015; Salinas et al., 2007, 2009), which will be beneficial for those targets with no “hotspot” (responders such as muscles). There are now easily operated toolkits to calculate the E-field vectors, which makes it possible to use the E-field to guide the coil direction in the future studies. The current study also used only a single session of intervention and had a small sample size. Ideally, we would recruit patients with PD to test and verify the current results, even if only a few patients. This is an objective for a future study.

6 | CONCLUSIONS

Low-frequency (1 Hz) rTMS to a site identified by fMRI finger-tapping activation significantly elevated the amplitude of local neural activity

(PerAF) in the ipsilateral putamen. The FC between the stimulation target and the basal ganglia was significantly enhanced following 1 Hz rTMS. These results suggested that low-frequency rTMS stimulation to a precisely localized individual finger-tapping task activation can modulate the local neural activity of the putamen (a pivotal brain region in PD) via FC. The current finding may provide a new insight into rTMS treatment in Parkinson's disease.

AUTHOR CONTRIBUTIONS

Jue Wang: Conceptualization, methodology, and formal analysis, Writing – original draft, Writing – review & editing, Funding acquisition. **Xin-Ping Deng:** Data collection and formal analysis, Writing – original draft. **Yun-Song Hu:** Validation. **Juan Yue:** Validation. **Qiu Ge:** Validation. **Xiao-Long Li:** Data collection. **Zi-Jian Feng:** Validation.

ACKNOWLEDGMENTS

We thank Liwen Bianji (Edanz) (www.liwenbianji.cn) for editing the language of a draft of this manuscript.

FUNDING INFORMATION

This work is supported by the Department of Science and Technology of Sichuan Province (No. 2022NSFSC0808); National Natural Science Foundation of China (No. 81701776).

CONFLICT OF INTEREST

The authors declared that they have no conflict of interest.

DATA AVAILABILITY STATEMENT

The data that support the findings of this study are available from the corresponding author upon reasonable request.

ORCID

Jue Wang  <https://orcid.org/0000-0003-4790-4827>

Zi-Jian Feng  <https://orcid.org/0000-0002-7228-3383>

REFERENCES

- Alexander, G. E., & Crutcher, M. D. (1990). Functional architecture of basal ganglia circuits: Neural substrates of parallel processing. *Trends in Neurosciences*, 13, 266–271.
- Arabkheradmand, G., Krieg, T. D., Salinas, F. S., Fox, P. T., & Mogul, D. J. (2019). Predicting TMS-induced activation in human neocortex using concurrent TMS/PET, finite element analysis and computational modeling. *Biomedical Physics and Engineering Express*, 5, 1–11.
- Ashburner, J. (2007). A fast diffeomorphic image registration algorithm. *NeuroImage*, 38, 95–113.
- Benninger, D. H. (2013). Brain stimulation: Chapter 37. Parkinson's disease. In *Handbook of clinical neurology* (Vol. 116, pp. 469–483). Elsevier.
- Bichsel, O., Gassert, R., Stieglitz, L., Uhl, M., Baumann-Vogel, H., Waldvogel, D., Baumann, C. R., & Imbach, L. L. (2018). Functionally separated networks for self-paced and externally-cued motor execution in Parkinson's disease: Evidence from deep brain recordings in humans. *NeuroImage*, 177, 20–29.
- Biswal, B., Yetkin, F. Z., Haughton, V. M., & Hyde, J. S. (1995). Functional connectivity in the motor cortex of resting human brain using echoplanar MRI. *Magnetic Resonance in Medicine*, 34, 537–541.
- Brabenec, L., Klobusiakova, P., Barton, M., Mekyska, J., Galaz, Z., Zvoncak, V., Kiska, T., Mucha, J., Smekal, Z., Kostalova, M., & Rektorova, I. (2019). Non-invasive stimulation of the auditory feedback area for improved articulation in Parkinson's disease. *Parkinsonism & Related Disorders*, 61, 187–192.
- Brooks, D. J., Salmon, E. P., Mathias, C. J., Quinn, N., Leenders, K. L., Bannister, R., Marsden, C. D., & Frackowiak, R. S. (1990). The relationship between locomotor disability, autonomic dysfunction, and the integrity of the striatal dopaminergic system in patients with multiple system atrophy, pure autonomic failure, and Parkinson's disease, studied with PET. *Brain*, 113(Pt 5), 1539–1552.
- Buzsaki, G., & Draguhn, A. (2004). Neuronal oscillations in cortical networks. *Science*, 304, 1926–1929.
- Carriere, N., Besson, P., Dujardin, K., Duhamel, A., Defebvre, L., Delmaire, C., & Devos, D. (2014). Apathy in Parkinson's disease is associated with nucleus accumbens atrophy: A magnetic resonance imaging shape analysis. *Movement Disorders*, 29, 897–903.
- Cash, R. F. H., Weigand, A., Zalesky, A., Siddiqi, S. H., Downar, J., Fitzgerald, P. B., & Fox, M. D. (2020). Using brain imaging to improve spatial targeting of transcranial magnetic stimulation for depression. *Biological Psychiatry*, 90, 689–700.
- Cho, S. S., Koshimori, Y., Aminian, K., Obeso, I., Rusjan, P., Lang, A. E., Daskalakis, Z. J., Houle, S., & Strafella, A. P. (2015). Investing in the future: Stimulation of the medial prefrontal cortex reduces discounting of delayed rewards. *Neuropsychopharmacology*, 40, 546–553.
- Chung, J. W., Burciu, R. G., Ofori, E., Coombes, S. A., Christou, E. A., Okun, M. S., Hess, C. W., & Vaillancourt, D. E. (2018). Beta-band oscillations in the supplementary motor cortex are modulated by levodopa and associated with functional activity in the basal ganglia. *NeuroImage: Clinical*, 19, 559–571.
- Cunnington, R., Windischberger, C., Deecke, L., & Moser, E. (2002). The preparation and execution of self-initiated and externally-triggered movement: A study of event-related fMRI. *NeuroImage*, 15, 373–385.
- Diekhoff, S., Uludag, K., Sparing, R., Tittgemeyer, M., Cavusoglu, M., von Cramon, D. Y., & Grefkes, C. (2011). Functional localization in the human brain: Gradient-Echo, spin-Echo, and arterial spin-labeling fMRI compared with neuronavigated TMS. *Human Brain Mapping*, 32, 341–357.
- Du, L., Liu, H., Du, W., Chao, F., Zhang, L., Wang, K., Huang, C., Gao, Y., & Tang, Y. (2018). Stimulated left DLPFC-nucleus accumbens functional connectivity predicts the anti-depression and anti-anxiety effects of rTMS for depression. *Translational Psychiatry*, 7, 3.
- Elahi, B., Elahi, B., & Chen, R. (2009). Effect of transcranial magnetic stimulation on Parkinson motor function—Systematic review of controlled clinical trials. *Movement Disorders*, 24, 357–363.
- Eldaief, M. C., Halko, M. A., Buckner, R. L., & Pascual-Leone, A. (2011). Transcranial magnetic stimulation modulates the brain's intrinsic activity in a frequency-dependent manner. *Proceedings of the National Academy of Sciences of the United States of America*, 108, 21229–21234.
- Esposito, F., Tessitore, A., Giordano, A., De Micco, R., Paccone, A., Conforti, R., Pignataro, G., Annunziato, L., & Tedeschi, G. (2013). Rhythm-specific modulation of the sensorimotor network in drug-naive patients with Parkinson's disease by levodopa. *Brain*, 136, 710–725.
- Feng, Z. J., Deng, X. P., Zhao, N., Jin, J., Yue, J., Hu, Y. S., Jing, Y., Wang, H. X., Knosche, T. R., Zang, Y. F., & Wang, J. (2021). Resting-state fMRI functional connectivity strength predicts local activity change in the dorsal cingulate cortex: A multi-target focused rTMS study. *Cerebral Cortex*, 32, 2773–2784.
- Fox, M. D., Snyder, A. Z., Vincent, J. L., Corbetta, M., Van Essen, D. C., & Raichle, M. E. (2005). The human brain is intrinsically organized into dynamic, anticorrelated functional networks. *Proceedings of the National Academy of Sciences of the United States of America*, 102, 9673–9678.

- Fox, P. T., Narayana, S., Tandon, N., Sandoval, H., Fox, S. P., Kochunov, P., & Lancaster, J. L. (2004). Column-based model of electric field excitation of cerebral cortex. *Human Brain Mapping*, 22, 1–14.
- Francois-Brosseau, F. E., Martinu, K., Strafella, A. P., Petrides, M., Simard, F., & Monchi, O. (2009). Basal ganglia and frontal involvement in self-generated and externally-triggered finger movements in the dominant and non-dominant hand. *The European Journal of Neuroscience*, 29, 1277–1286.
- Friston, K. J., Frith, C. D., Liddle, P. F., & Frackowiak, R. S. (1993). Functional connectivity: The principal-component analysis of large (PET) data sets. *Journal of Cerebral Blood Flow and Metabolism*, 13, 5–14.
- Friston, K. J., Williams, S., Howard, R., Frackowiak, R. S., & Turner, R. (1996). Movement-related effects in fMRI time-series. *Magnetic Resonance in Medicine*, 35, 346–355.
- Herz, D. M., Eickhoff, S. B., Lokkegaard, A., & Siebner, H. R. (2014). Functional neuroimaging of motor control in Parkinson's disease: A meta-analysis. *Human Brain Mapping*, 35, 3227–3237.
- Hikosaka, O., Takikawa, Y., & Kawagoe, R. (2000). Role of the basal ganglia in the control of purposive saccadic eye movements. *Physiological Reviews*, 80, 953–978.
- Ji, G. J., Yu, F., Liao, W., & Wang, K. (2017). Dynamic aftereffects in supplementary motor network following inhibitory transcranial magnetic stimulation protocols. *NeuroImage*, 149, 285–294.
- Jia, X. Z., Sun, J. W., Ji, G. J., Liao, W., Lv, Y. T., Wang, J., Wang, Z., Zhang, H., Liu, D. Q., & Zang, Y. F. (2020). Percent amplitude of fluctuation: A simple measure for resting-state fMRI signal at single voxel level. *PLoS One*, 15, e0227021.
- Jia, X. Z., Wang, J., Sun, H. Y., Zhang, H., Liao, W., Wang, Z., Yan, C. G., Song, X. W., & Zang, Y. F. (2019). RESTplus an improved toolkit for resting-state functional magnetic resonance imaging data processing. *Science Bulletin*, 64, 953–954.
- Khedr, E. M., Al-Fawal, B., Abdel Wraith, A., Saber, M., Hasan, A. M., Bassiony, A., Nasr Eldein, A., & Rothwell, J. C. (2019). The effect of 20 Hz versus 1 Hz repetitive transcranial magnetic stimulation on motor dysfunction in Parkinson's disease: Which is more beneficial? *Journal of Parkinson's Disease*, 9, 379–387.
- Kim, M. S., Chang, W. H., Cho, J. W., Youn, J., Kim, Y. K., Kim, S. W., & Kim, Y. H. (2015). Efficacy of cumulative high-frequency rTMS on freezing of gait in Parkinson's disease. *Restorative Neurology and Neuroscience*, 33, 521–530.
- Krieg, T. D., Salinas, F. S., Narayana, S., Fox, P. T., & Mogul, D. J. (2013). PET-based confirmation of orientation sensitivity of TMS-induced cortical activation in humans. *Brain Stimulation*, 6, 898–904.
- Krieg, T. D., Salinas, F. S., Narayana, S., Fox, P. T., & Mogul, D. J. (2015). Computational and experimental analysis of TMS-induced electric field vectors critical to neuronal activation. *Journal of Neural Engineering*, 12, 046014.
- Lee, S. Y., Kim, M. S., Chang, W. H., Cho, J. W., Youn, J. Y., & Kim, Y. H. (2014). Effects of repetitive transcranial magnetic stimulation on freezing of gait in patients with parkinsonism. *Restorative Neurology and Neuroscience*, 32, 743–753.
- Lefaucheur, J. P. (2009). Treatment of Parkinson's disease by cortical stimulation. *Expert Review of Neurotherapeutics*, 9, 1755–1771.
- Lefaucheur, J. P. (2019). Transcranial magnetic stimulation. *Handbook of Clinical Neurology*, 160, 559–580.
- Lefaucheur, J. P., Andre-Obadia, N., Antal, A., Ayache, S. S., Baeken, C., Benninger, D. H., Cantello, R. M., Cincotta, M., de Carvalho, M., De Ridder, D., Devanne, H., Di Lazzaro, V., Filipovic, S. R., Hummel, F. C., Jaaskelainen, S. K., Kimiskidis, V. K., Koch, G., Langguth, B., Nyffeler, T., ... Garcia-Larrea, L. (2014). Evidence-based guidelines on the therapeutic use of repetitive transcranial magnetic stimulation (rTMS). *Clinical Neurophysiology*, 125, 2150–2206.
- Lefaucheur, J. P., Drouot, X., Von Raison, F., Menard-Lefaucheur, I., Cesaro, P., & Nguyen, J. P. (2004). Improvement of motor performance and modulation of cortical excitability by repetitive transcranial magnetic stimulation of the motor cortex in Parkinson's disease. *Clinical Neurophysiology*, 115, 2530–2541.
- Li, Z. J., Wu, Q., & Yi, C. J. (2015). Clinical efficacy of istradefylline versus rTMS on Parkinson's disease in a randomized clinical trial. *Current Medical Research and Opinion*, 31, 2055–2058.
- Lisanby, S. H., Gutman, D., Luber, B., Schroeder, C., & Sackeim, H. A. (2001). Sham TMS: Intracerebral measurement of the induced electrical field and the induction of motor-evoked potentials. *Biological Psychiatry*, 49, 460–463.
- Liu, C., Dai, Z., Zhang, R., Zhang, M., Hou, Y., Qi, Z., Huang, Z., Lin, Y., Zhan, S., He, Y., & Wang, Y. (2015). Mapping intrinsic functional brain changes and repetitive transcranial magnetic stimulation neuro-modulation in idiopathic restless legs syndrome: A resting-state functional magnetic resonance imaging study. *Sleep Medicine*, 16, 785–791.
- Ma, J., Gao, L., Mi, T., Sun, J., Chan, P., & Wu, T. (2019). Repetitive transcranial magnetic stimulation does not improve the sequence effect in freezing of gait. *Parkinson's Disease*, 2019, 2196195.
- McGregor, M. M., & Nelson, A. B. (2019). Circuit mechanisms of Parkinson's disease. *Neuron*, 101, 1042–1056.
- Mi, T. M., Garg, S., Ba, F., Liu, A. P., Wu, T., Gao, L. L., Dan, X. J., Chan, P., & McKeown, M. J. (2019). High-frequency rTMS over the supplementary motor area improves freezing of gait in Parkinson's disease: A randomized controlled trial. *Parkinsonism & Related Disorders*, 68, 85–90.
- Middleton, F. A., & Strick, P. L. (2000). Basal ganglia and cerebellar loops: Motor and cognitive circuits. *Brain Research. Brain Research Reviews*, 31, 236–250.
- Mink, J. W. (2006). Neurobiology of basal ganglia and Tourette syndrome: Basal ganglia circuits and thalamocortical outputs. *Advances in Neurology*, 99, 89–98.
- Nicola, S. M. (2007). The nucleus accumbens as part of a basal ganglia action selection circuit. *Psychopharmacology*, 191, 521–550.
- O'Boyle, D. J., Freeman, J. S., & Cody, F. W. (1996). The accuracy and precision of timing of self-paced, repetitive movements in subjects with Parkinson's disease. *Brain*, 119(Pt 1), 51–70.
- Opitz, A., Legon, W., Rowlands, A., Bickel, W. K., Paulus, W., & Tyler, W. J. (2013). Physiological observations validate finite element models for estimating subject-specific electric field distributions induced by transcranial magnetic stimulation of the human motor cortex. *NeuroImage*, 81, 253–264.
- Packard, M. G., & Knowlton, B. J. (2002). Learning and memory functions of the basal ganglia. *Annual Review of Neuroscience*, 25, 563–593.
- Pascual-Leone, A., Amedi, A., Fregni, F., & Merabet, L. B. (2005). The plastic human brain cortex. *Annual Review of Neuroscience*, 28, 377–401.
- Pascual-Leone, A., Tormos, J. M., Keenan, J., Tarazona, F., Canete, C., & Catala, M. D. (1998). Study and modulation of human cortical excitability with transcranial magnetic stimulation. *Journal of Clinical Neurophysiology*, 15, 333–343.
- Playford, E. D., Jenkins, I. H., Passingham, R. E., Nutt, J., Frackowiak, R. S., & Brooks, D. J. (1992). Impaired mesial frontal and putamen activation in Parkinson's disease: A positron emission tomography study. *Annals of Neurology*, 32, 151–161.
- Rossini, P. M., Burke, D., Chen, R., Cohen, L. G., Daskalakis, Z., Di Iorio, R., Di Lazzaro, V., Ferreri, F., Fitzgerald, P. B., George, M. S., Hallett, M., Lefaucheur, J. P., Langguth, B., Matsumoto, H., Miniussi, C., Nitsche, M. A., Pascual-Leone, A., Paulus, W., Rossi, S., ... Ziemann, U. (2015). Non-invasive electrical and magnetic stimulation of the brain, spinal cord, roots and peripheral nerves: Basic principles and procedures for routine clinical and research application. An updated report from an I.F.C.N. Committee. *Clinical Neurophysiology*, 126, 1071–1107.
- Salinas, F. S., Franklin, C., Narayana, S., Szabo, C. A., & Fox, P. T. (2016). Repetitive transcranial magnetic stimulation educes frequency-specific causal relationships in the motor network. *Brain Stimulation*, 9, 406–414.

- Salinas, F. S., Lancaster, J. L., & Fox, P. T. (2007). Detailed 3D models of the induced electric field of transcranial magnetic stimulation coils. *Physics in Medicine and Biology*, *52*, 2879–2892.
- Salinas, F. S., Lancaster, J. L., & Fox, P. T. (2009). 3D modeling of the total electric field induced by transcranial magnetic stimulation using the boundary element method. *Physics in Medicine and Biology*, *54*, 3631–3647.
- Salinas, F. S., Narayana, S., Zhang, W., Fox, P. T., & Szabo, C. A. (2013). Repetitive transcranial magnetic stimulation elicits rate-dependent brain network responses in non-human primates. *Brain Stimulation*, *6*, 777–787.
- Saravanamuttu, J., Radhu, N., Udupa, K., Baarbe, J., Gunraj, C., & Chen, R. (2021). Impaired motor cortical facilitatory-inhibitory circuit interaction in Parkinson's disease. *Clinical Neurophysiology*, *132*, 2685–2692.
- Speer, A. M., Kimbrell, T. A., Wassermann, E. M., Repella, J. D., Willis, M. W., Herscovitch, P., & Post, R. M. (2000). Opposite effects of high and low frequency rTMS on regional brain activity in depressed patients. *Biological Psychiatry*, *48*, 1133–1141.
- Strafella, A. P., Paus, T., Barrett, J., & Dagher, A. (2001). Repetitive transcranial magnetic stimulation of the human prefrontal cortex induces dopamine release in the caudate nucleus. *The Journal of Neuroscience*, *21*, RC157.
- Taniwaki, T., Okayama, A., Yoshiura, T., Togao, O., Nakamura, Y., Yamasaki, T., Ogata, K., Shigetou, H., Ohyagi, Y., Kira, J., & Tobimatsu, S. (2006). Functional network of the basal ganglia and cerebellar motor loops in vivo: Different activation patterns between self-initiated and externally triggered movements. *NeuroImage*, *31*, 745–753.
- Tzourio-Mazoyer, N., Landeau, B., Papathanassiou, D., Crivello, F., Etard, O., Delcroix, N., Mazoyer, B., & Joliot, M. (2002). Automated anatomical labeling of activations in SPM using a macroscopic anatomical parcellation of the MNI MRI single-subject brain. *NeuroImage*, *15*, 273–289.
- Vidal-Pineiro, D., Martin-Trias, P., Falcon, C., Bargallo, N., Clemente, I. C., Valls-Sole, J., Junque, C., Pascual-Leone, A., & Bartres-Faz, D. (2015). Neurochemical modulation in posteromedial default-mode network cortex induced by transcranial magnetic stimulation. *Brain Stimulation*, *8*, 937–944.
- Wang, J., Deng, X. P., Wu, Y. Y., Li, X. L., Feng, Z. J., Wang, H. X., Jing, Y., Zhao, N., Zang, Y. F., & Zhang, J. (2020). High-frequency rTMS of the motor cortex modulates cerebellar and widespread activity as revealed by SVM. *Frontiers in Neuroscience*, *14*, 186.
- Wang, J., Meng, H. J., Ji, G. J., Jing, Y., Wang, H. X., Deng, X. P., Feng, Z. J., Zhao, N., Zang, Y. F., & Zhang, J. (2019). Finger tapping task activation vs. TMS hotspot: Different locations and networks. *Brain Topography*, *33*, 123–134.
- Wang, J., Zhang, J. R., Zang, Y. F., & Wu, T. (2018). Consistent decreased activity in the putamen in Parkinson's disease: A meta-analysis and an independent validation of resting-state fMRI. *Gigascience*, *7*(6), giy071.
- Wang, J. X., Rogers, L. M., Gross, E. Z., Ryals, A. J., Dokucu, M. E., Brandstatt, K. L., Hermiller, M. S., & Voss, J. L. (2014). Targeted enhancement of cortical-hippocampal brain networks and associative memory. *Science*, *345*, 1054–1057.
- Wang, Z., Liang, S., Yu, S., Xie, T., Wang, B., Wang, J., Li, Y., Shan, B., & Cui, C. (2017). Distinct roles of dopamine receptors in the lateral thalamus in a rat model of decisional impulsivity. *Neuroscience Bulletin*, *33*, 413–422.
- Watanabe, T., Hanajima, R., Shirota, Y., Tsutsumi, R., Shimizu, T., Hayashi, T., Terao, Y., Ugawa, Y., Katsura, M., Kunimatsu, A., Ohtomo, K., Hirose, S., Miyashita, Y., & Konishi, S. (2015). Effects of rTMS of pre-supplementary motor area on fronto basal ganglia network activity during stop-signal task. *The Journal of Neuroscience*, *35*, 4813–4823.
- Wu, A. D., Fregni, F., Simon, D. K., Deblieck, C., & Pascual-Leone, A. (2008). Noninvasive brain stimulation for Parkinson's disease and dystonia. *Neurotherapeutics*, *5*, 345–361.
- Wu, T., Long, X., Zang, Y., Wang, L., Hallett, M., Li, K., & Chan, P. (2009). Regional homogeneity changes in patients with Parkinson's disease. *Human Brain Mapping*, *30*, 1502–1510.
- Xia, M., Wang, J., & He, Y. (2013). BrainNet viewer: A network visualization tool for human brain connectomics. *PLoS One*, *8*, e68910.
- Xue, S. W., Guo, Y., Peng, W., Zhang, J., Chang, D., Zang, Y. F., & Wang, Z. (2017). Increased low-frequency resting-state brain activity by high-frequency repetitive TMS on the left dorsolateral prefrontal cortex. *Frontiers in Psychology*, *8*, 2266.
- Yan, C. G., Cheung, B., Kelly, C., Colcombe, S., Craddock, R. C., Di Martino, A., Li, Q., Zuo, X. N., Castellanos, F. X., & Milham, M. P. (2013). A comprehensive assessment of regional variation in the impact of head micromovements on functional connectomics. *NeuroImage*, *76*, 183–201.
- Yan, C. G., Wang, X. D., Zuo, X. N., & Zang, Y. F. (2016). DPABI: Data Processing & Analysis for (resting-state) brain imaging. *Neuroinformatics*, *14*, 339–351.
- Yin, H. H., & Knowlton, B. J. (2006). The role of the basal ganglia in habit formation. *Nature Reviews. Neuroscience*, *7*, 464–476.
- Yousry, T. A., Schmid, U. D., Alkadhi, H., Schmidt, D., Peraud, A., Buettner, A., & Winkler, P. (1997). Localization of the motor hand area to a knob on the precentral gyrus. A new landmark. *Brain*, *120*(Pt 1), 141–157.
- Zhao, N., Yuan, L. X., Jia, X. Z., Zhou, X. F., Deng, X. P., He, H. J., Zhong, J., Wang, J., & Zang, Y. F. (2018). Intra- and inter-scanner reliability of voxel-wise whole-brain analytic metrics for resting state fMRI. *Frontiers in Neuroinformatics*, *12*, 54.
- Zuo, X. N., Di Martino, A., Kelly, C., Shehzad, Z. E., Gee, D. G., Klein, D. F., Castellanos, F. X., Biswal, B. B., & Milham, M. P. (2010). The oscillating brain: Complex and reliable. *NeuroImage*, *49*, 1432–1445.

SUPPORTING INFORMATION

Additional supporting information can be found online in the Supporting Information section at the end of this article.

How to cite this article: Wang, J., Deng, X.-P., Hu, Y.-S., Yue, J., Ge, Q., Li, X.-L., & Feng, Z.-J. (2023). Low-frequency rTMS targeting individual self-initiated finger-tapping task activation modulates the amplitude of local neural activity in the putamen. *Human Brain Mapping*, *44*(1), 203–217. <https://doi.org/10.1002/hbm.26045>